PRINCIPLES OF RAPID POLYMERASE CHAIN REACTION: MATHEMATICAL MODELING AND EXPERIMENTAL VERIFICATION

H. J. Viljoen, R.M. Nelson[1], S. Whitney
Department of Chemical Engineering, University of Nebraska, Lincoln, NE 68588, U.S.A.
[1] Megabase Research products, 4700 Huntington Ave., Lincoln, NE 68514 U.S.A.

1. Introduction

Polymerase Chain Reaction. The development of the polymerase chain reaction (PCR) to amplify a nucleic acid sequence has found widespread applications in molecular biology (Saiki *et al*., 1985, Mullis and Faloona 1987). The amplification of a DNA sample by PCR consists of three steps. The first stage in the PCR amplification process is separation (denaturation) of the double stranded DNA (dsDNA) at elevated temperatures (typically 90°C-95°C) to form single stranded DNA (ssDNA). Next sequence-specific primers attach (anneal) to the resultant ssDNA molecules at lowered temperatures (50°C-65°C). Finally the primers are extended (elongation) enzymatically to create copies of the original DNA (at ~72°C). When these stages are repeated, the DNA concentration increases dramatically.

Batch Reactor. Most PCR reactions are performed in 10-50 µl reaction volumes. These non-isothermal systems are closed and, therefore, are modeled as batch reactors. Unfortunately there is paucity in detailed kinetic data. However, it is known that annealing is favored at lower temperatures and denaturation is favored at elevated temperatures. With the temperatures typically used in PCR, one can assume denaturation does not occur at the annealing temperature and that annealing does not occur at the denaturation temperature. The elongation rate is faster at elevated temperatures; at the annealing temperature the elongation rate is typically negligible. Yet, if the temperature is too high (such as near the denaturation temperature) the polymerase falls off the primer-target template and elongation ceases. The thermal cycling of the cuvets and their contents is affected by a thermocycler.

PCR Reactors. Also known as thermocyclers, several designs have been proposed over the past two decades. A variety of machines have been built which automate the three-step PCR amplification process (Oste, 1989; Oste, 1994; Newton, 1995; Johnson, 1998). Generally, these devices may be classified into two categories: *robotic devices* which move the DNA samples to the heat; and *thermocyclers* which bring the heat to the samples. Robotic devices such as Stratagene's ROBOCYCLER™ move tubes containing PCR reaction samples to and from a series of water baths, which are heated to different temperatures. Although robotic thermocyclers may be useful in certain research applications, they are incapable of high-speed PCR. They require >60 minutes for 30 cycles of DNA amplification; equivalent to >2 minutes per PCR cycle. Since the late 1980s, thermocyclers have become familiar devices in many biochemistry laboratories. In general, two types of thermocyclers are employed: *programmable heat blocks* and *forced hot-air thermocyclers*. Most thermocyclers are programmable heat blocks with holes in them where thin-walled plastic reaction tubes are heated and cooled under electronic control. Several such devices have been reviewed by Johnson (1998). The problem is that most of the time is spent waiting for a bulky piece of metal to heat up or cool down. To overcome the long transitional dead times of heat blocks, forced hot-air thermocyclers have been constructed. In commercial hot-air thermocyclers, first built by Idaho Technology (Rapid Cycler™; Idaho Falls, Idaho, USA) and subsequently by Roche Diagnostics Corporation (LightCycler™; Penzburg, Germany) the time needed for one PCR cycle of

denaturation/annealing/elongation was substantially reduced because: (1) heat transfer from forced hot air to the aqueous biochemical reaction sample was carried out in thin-walled capillary tubes; (2) the reaction chamber had very low thermal mass; and (3) the denaturation and annealing times during the PCR cycle were reduced. Nicoll *et al.* (2001) amplified (96 to 220 b.p.) herpes virus DNA fragments through 50 PCR cycles of [0 sec 94ºC (denaturation), 3 sec 58º to 67ºC (annealing), 6 sec 72ºC (elongation)] in ~25 minutes; or about 30 seconds/cycle using a Roche LightCycler™.

In our laboratory we have built pressurized air thermocyclers (PCRJet™) that perform typically five times faster than the forced hot-air thermocyclers. Based on computational fluid dynamics, the convective heat transfer to and from cuvets has been optimized by using pressurized gases. In Fig.1 the output, as shown on the computer screen is shown. The machine completed thirty cycles in 42 seconds; or 1.4 seconds/cycle. This machine is by far the fastest thermocycler described to date. Although 1.4 seconds/cycle is too fast for any biochemistry, it shows that the time limiting process is biochemistry and not the device. As a further demonstration of our thermocycler,s performance, the results of ~10^8-fold amplification of a 368 base pair diagnostic *Bacillus anthracis* DNA fragment is shown in Fig.2. It was achieved using 30 PCR cycles in <4 minutes. The PCRJet™ thermocycler has set speed records for every DNA amplicon tested. In general, viral and bacterial DNA fragments 100 to 500 b.p. long were typically amplified through 30 PCR cycles in 2 to 4 minutes; whereas single copy human gene fragments in this size range required ~3,5 to 6,0 minutes for 35 PCR cycles.

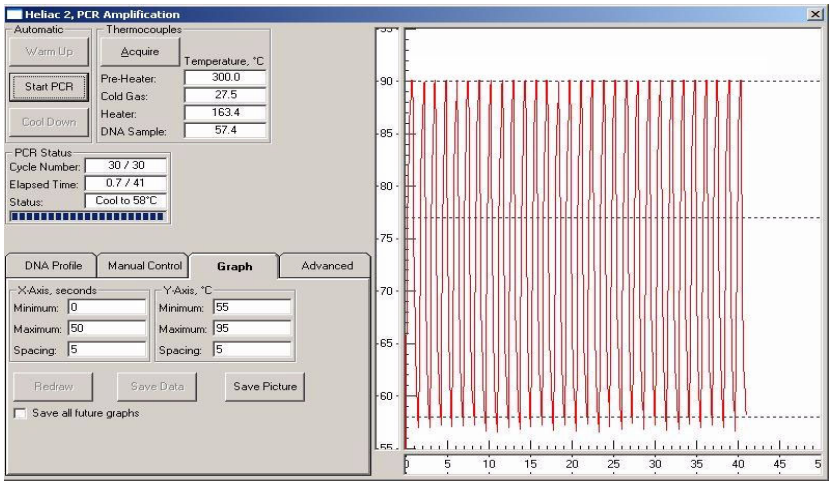

Figure 1: Temperature vs. time (seconds) output for ultra-fast thermo-cycling in our PCRJet.

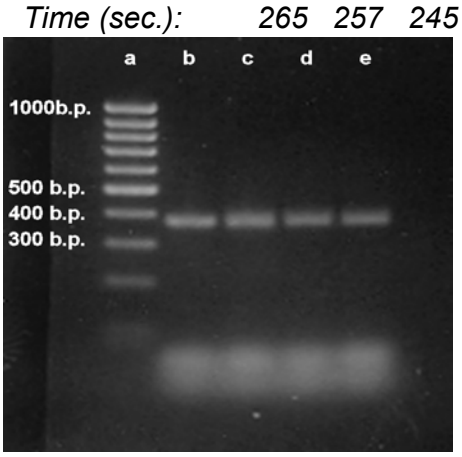

Figure 2: High-speed amplification of 368 b.p. Bacillus anthracis DNA fragment in PCRJet. 10 pg of DNA from B. anthracis Sterne strain were amplified in a 16 ul PCR reaction in a 1 mm OD glass capillary tube containing 1.25 U KOD HotStart DNA Pol (Toyobo Co. Ltd), 1 uM 21mer oligonucleotide primers, 3.5 mM Mg++, and 500 ug/ml BSA. After PCR, DNA fragments were separated on a 2% agarose gel and stained using 0.7 ug/ml EtBr. M.W. markers are in lane [a]. 30 cycles of PCR were carried out using: [b] [0 sec 92C, 0 sec 55C, 4.2 sec 72C], [c] [0 sec 92C, 0 sec 55C, 3.8 sec 72C], [d] [0 sec 92C, 0 sec 55C, 3.5 sec 72C], [e] [0 sec 92C, 0 sec 55C, 3.2 sec 72C]. In lane [e] the total time needed for 10^8-fold amplification of the 368 bp B.anthracis amplicon was 3 minutes, 53 seconds (233 seconds).

Key to the fast operation is the combination of effective heat transfer and the small size of the cuvet, which can be viewed as a micro batch reactor. However, it is important not to miniaturize at the expense of performance. Theoretically, the amplified nucleic acid concentration should double after each cycle. In practice, the DNA does not increase by a factor of two after each cycle. Instead, the DNA increases by a factor of $(1+Y)$ where Y is the cycle efficiency. Thus an efficiency of $Y = 100\%$ would imply a doubling of the DNA concentration. The cycles are repeated n times until the concentrations are sufficient for detection; thirty to forty PCR cycles are typical. It is customary to report overall efficiency and overall yield over the n cycles instead of efficiency and yield after every cycle. Saiki *et al*. (1985) related the overall efficiency (Y) and yield (X) as follows: $X = (1+Y)^n$ and this relation became the standard way to express the overall efficiency[1] of PCR processes (Keohavang *et al*., 1988, Li *et al*., 1988). A small variation on this relation has been proposed by Newton and Graham (1997) if the original DNA is genomic DNA with a length greater than the target DNA length It has been experimentally observed that yields could vary from cycle to cycle with the general trend to decrease with increasing cycle numbers (Kainz (2000), Schnell and Mendoza (1997a, 1997b), Stolovitzky and Cecchi (1996).

Additional references are listed in Waterfall, Eisenthal and Cobb (2002)). Gilliland *et al*. (1990) ascribed the drop in efficiency to consumption of primers and dNTPs, production of pyrophosphates that promotes the reverse pyrophosphorolysis reaction and other

---

[1] The efficiency Y in the equation $X = (1+Y)^n$ has frequently been erroneously reported as the average of the individual cycle efficiencies. Suppose two cycles are performed at 50% and 100% efficiency respectively. These two cycles increase the DNA concentration by a factor $(1+50\%)(1+100\%) = 3$; the overall efficiency is $Y = 3^{1/2} - 1 = 73.2\%$ which is smaller than the average cycle efficiency of 75%.

factors. They noted that efficiency could vary substantially among identical samples, prepared with master mixes.

In light of this discussion, the need of a mathematical model to optimize yield in the micro reactors is obvious. Next the experimental methods are briefly described that have been used to verify the results of the mathematical model, followed by a description of the mathematical model and a comparison between the model and experiments.

2. Experimental Methods

The mathematical model describes the progression of the whole process and can determine the overall yield. The calculated yield is compared, below, to experimental values. For that purpose three different sized amplicons have been selected; *Escherichia coli*-297bp, *Bacillus cereus*–600bp, and bacteriophage λ-2206bp. For each amplicon two different polymerases have been used: *Thermus aquaticus* (*Taq*) polymerase and *Thermococcus kodakaraensis* (KOD) polymerase; a total of six experimental yields are reported. Each experiment has been repeated five times and the yields are the average values.

The experimental yields are determined as follows. The initial DNA concentration is C_0 and the amplified DNA concentration is determined by gel electrophoresis, denoted as C_P. The target DNA has a total of N_T base pairs and the amplicon (a fraction of the target) has N_A base pairs. The overall yield Y is given by:

$$[1+Y]^n = (C_P / C_0)(N_T / N_A).$$

a. Materials and Methods:

A 25 □l volume of PCR reaction mixture has been prepared from:

- fractional volumes of 1 unit/□l of KOD hot start polymerase or *Taq* polymerase,
- 10X KOD hot start polymerase buffer (Novagen, Wisconsin, Madison) or *Taq* buffer (Idaho Technologies, ID),
- dye consisting of 10X sucrose and cresol (Idaho Technologies, ID),
- bovine serum albumin (BSA, Sigma chemicals, St. Louis, MO),
- 4 mM MgSO4,
- 200 □M deoxynucleotide tri-phosphate (dNTP),
- 1:1 ratio of 1 □M reverse primers and 1 □M forward primers,
- 3 □M dUTPase for □DNA, and
- 10 pg to 10 ng of *E. coli*, *Bacillus cereus* and bacteriophage □DNA as required (see Table I).

After the PCR mix has been amplified, it is subjected to gel electrophoresis. The concentration of the amplified DNA is measured by comparison to known amounts DNA molecular weight markers after ethidium bromide staining. For further details on experimental method, see Whitney et al. (2004).

Thermocycler. The DNA is amplified in the PCRJet™ thermocycler (Quintanar and Nelson, U.S. Pat. 6,472,186). The speed of the machine is better utilized in combination with a faster enzyme, such as KOD polymerase. KOD polymerase requires an initial 30 seconds hot start at 90°C to fully activate the KOD polymerase – which is a pair of antibodies which

thermally denature at ~80°C. Fig.1 shows the temperature-time plot over thirty cycles for a typical PCRJet run. The temperature plateau for the first 30 seconds is the hot start period. During this period thermolabile antibodies bound to the DNA polymerase are inactivated (cf. Mizuguchi et al. (1999)). The PCRJet has been programmed for a 2 second elongation time. The elongation speed of the KOD polymerase has been measured to be approximately 300 nt/s and the temperature protocol shown in Fig.1 would amplify amplicons of length $N_T < 600$ base pairs. It must be noted that KOD polymerase is sufficiently fast to accomplish elongation for shorter amplicons during ramping from annealing to denaturation without the need to pause at an elongation temperature. Fig.1b shows a case where no pause for extension is programmed.

No hot start is required for the *Taq* polymerase, but it has a considerably slower extension rate than the KOD polymerase. Innis *et al.*, (1988) and Gelfand and White, (1990) reported $v \approx 80$ nt/s for *Taq pol*. However, this is an apparent rate that did not distinguish between the true time for extension and the total time to anneal and extend. The rate for *Taq pol*, after correction for the annealing time, is closer to 110 nt/s.

3. Mathematical Model

The model consists of three parts: denaturation of DNA, primer-template annealing and elongation. The three stages are schematically presented in Fig.3. In the following section these steps are discussed.

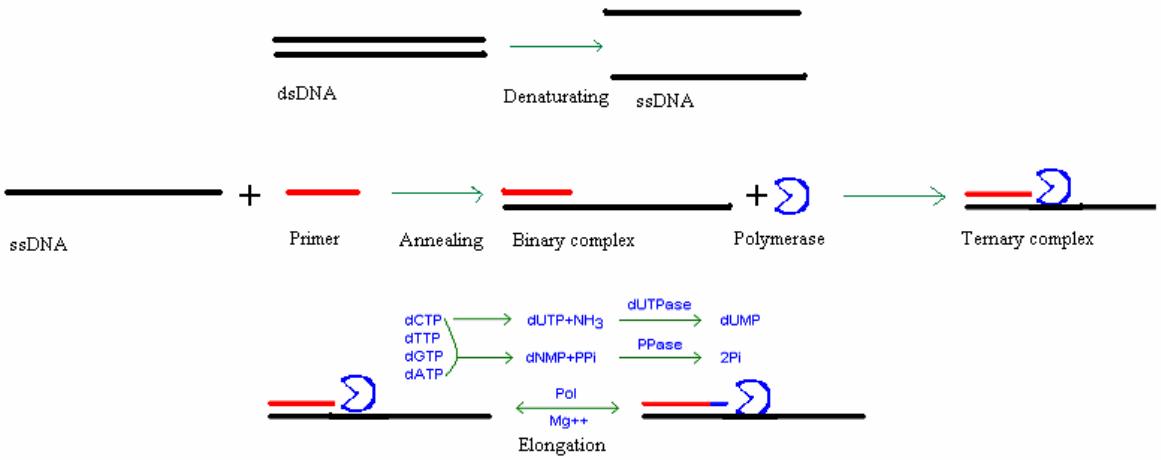

Figure. 3: Schematic reaction scheme of PCR

b. Denaturation

The first step in the PCR process is denaturation of the double-stranded DNA at elevated temperatures (Fig.3, top). The model assumes denaturation is complete if the temperature is raised sufficiently.

The initial amounts of all species are scaled by the initial number of DNA copies. Thus the scaled number of DNA molecules is always one at the start. To illustrate this point, consider an initial amount of 2×10^{14} dNTP molecules. If the initial number of DNA copies is 100, then the model scales the values to 1 copy of DNA and 2×10^{12} molecules of dNTP. At any cycle, the DNA concentration before the denaturation step is denoted by D. The reaction (1) below describes the denaturing of double-stranded DNA into single-stranded DNA complementary molecules. Note that the variables used in the reaction scheme are also the variables used in the mathematical model. This approach is followed throughout

this paper.

$$D \rightarrow d_1 + d_2 . \qquad (1)$$

The time allocated for denaturation is t_D. Therefore we can write at the end of the denaturation step:

$$D = 0, d_1 = D, d_2 = D , \quad \text{at } t = t_D .$$

The polymerase enzyme, ε, is damaged by exposure to high temperature. This phenomenon is described in the model by a damage factor $k_D \times t_D$ (Illanes and Wilson (2003)). The thermal deactivation model is:

$$\frac{d\varepsilon}{dt} = -k_D \varepsilon .$$

The amount of polymerase that still remains active at the end of the denaturation period is:

$$\varepsilon(t_D) = \varepsilon(0) e^{-k_D t_D} . \qquad (2)$$

The only problem is to find reliable values for k_D. In this paper we have assumed $e^{-k_D t_D}$ = 0.98; thus 2% of the polymerase is irreversibly damaged during each denaturation step. In the simulations we have done to compare the results with experimental findings, excess of polymer has been used. Despite the loss of polymerase, it is still in excess and the reaction does not become inhibited on that account. However, it makes the model more general and it can be used to study the inhibitive role of polymerase shortage.

c. Annealing

At the start of the annealing step (Fig.3, middle), we reset time to $t = 0$. The length of the amplicon is denoted as N_A base pairs, excluding the length of the primer. For example, if a primer of length 12 bp is used to amplify a 286 bp amplicon, $N_A = 286\ \text{bp} - 12\ \text{bp} = 274\ \text{bp}$. The reactions between primers and target strands, as well as the undesirable self-annealing of DNA strands are shown in Eqs. (3a-c).

$$d_2 + p_1(i) \rightarrow p1d(i)$$
$$d_1 + p_2(i) \rightarrow p2d(i) \qquad (3a-c)$$
$$d_1 + d_2 \rightarrow D$$

Eqns. (3a,b) describe chemical reactions for the annealing of primers $p_1(i)$ and $p_2(i)$ to ssDNA molecules d_2 and d_1 respectively. Likewise eq. (3c) describes the annealing of two full-length ssDNA molecules to form a dsDNA duplex D. According to the notation, the primers and $p_{1,2}(i)$ $(1 \le i < N_A)$ denote strands that have extended partially during a previous cycle. Some of these intermediaries may have low concentrations, but they do form, especially if the elongation time is short or reactants are depleted. Thus the first two reactions (3a,b) describe the formation of primer-template complexes and the third reaction accounts for recombination of template strands. Statistically the last reaction has low probability. The reactions (3a,b) would dominate, since the primer concentrations far exceed the target DNA concentration, but towards the last few cycles the DNA concentration may become appreciable and thence reaction (3c) should be included in the analysis. For the purpose of the model, the same rate constant k_A is used for all reactions (3a-c). This may be viewed as a limitation, but it offers us mathematical expediency. On the other hand, if kinetic data are published that clearly show huge differences in the rate constants, it would be straightforward to include that in the model.

A complication that may arise during the annealing step is primer-primer interaction. We include the possibility that annealing may occur between primers of all lengths $0 \le i < N_A - 1$

(Note that $i=N_A$ is equivalent to $d_{1,2}$ and is therefore described by reactions (3a,b)). Primers of length $0 < i < N_A$ are of course a result of incomplete elongation during a prior cycle. These interactions are described by:

$$p_1(i) + p_2(j) \rightarrow p12(i,j). \quad (4)$$

The same rate constant k_P is used for all reactions in (4), a reasonable assumption for a qualitative model. The rate expressions for the *i*th reactions in (3a,b) are:

$$\frac{dp_1(i)}{dt} = -k_A p_1(i) d_2 - k_P p_1(i) \sum_0^{N_A-1} p_2(j)$$

$$\frac{dp_2(i)}{dt} = -k_A p_2(i) d_1 - k_P p_2(i) \sum_0^{N_A-1} p_1(j).$$

The fragments of length *i*, $p_1(i)$ and $p_2(i)$, react with single-stranded DNA d_2 and d_1 respectively. The first terms on the right hand side of the above equations describe these contributions. The second terms on the right hand side account for the reactions of $p_1(i)$ and $p_2(i)$ with all complementary fragments of lengths *j*=0 to *j*=*N*-1.

Substitute $p_{tk} = \sum_{i=0}^{N_A-1} p_k(i)$ (for *k*=1,2) in the above rate expressions and take the sum over all rate expressions (*i*=0,..N_A-1) to obtain:

$$\frac{dp_{t1}}{dt} = -k_A p_{t1} d_2 - k_P p_{t1} p_{t2}. \quad (5a)$$

$$\frac{dp_{t2}}{dt} = -k_A p_{t2} d_1 - k_P p_{t2} p_{t1}. \quad (5b)$$

The rate of change of d_1 from eq.(3c) is given by the following equation:

$$\frac{dd_1}{dt} = -k_A \left[p_{t2} d_1 + d_1 d_2 \right]. \quad (6)$$

Symmetry[2] assures that for all time t, $d_1 = d_2$ and $p_{t1} = p_{t2}$ and eqns. (5,6) are written as follows:

$$\frac{dp_{t1}}{dt} = -k_A p_{t1} d_1 - k_P p_{t1}^2, \quad (7)$$

$$\frac{dd_1}{dt} = -k_A \left[p_{t1} d_1 + d_1^2 \right]. \quad (8)$$

Let $\gamma = k_P / k_A$ and $z = d_1 / p_{t1}$, also let $p_{t1}(0)$, $d_1(0)$ denote the values at the onset of the annealing step. It follows from Eqs.(7-8) that

$$\frac{dd_1}{dp_{t1}} = \frac{z(z+1)}{z+\gamma} = z + p_{t1} \frac{dz}{dp_{t1}}.$$

The solution is trivial if $\gamma = 1$, $\frac{d_1}{p_{t1}} = \frac{d_1(0)}{p_{t1}(0)}$.

For $\gamma \neq 1$, the solution is:

$$\frac{d_1}{p_{t1}} - \frac{d_1(0)}{p_{t1}(0)} + \gamma \ln\left(\frac{d_1}{d_1(0)} \right) = \ln\left(\frac{p_{t1}}{p_{t1}(0)} \right).$$

---

[2] Even in stochastic processes (and the extension step is treated as such), this equivalence would reflect the most likely outcome.

When the logarithmic terms are expanded to second order in their Laurent series representations, one can write:

$$p_{t1} = \frac{d_1 p_{t1}(0)}{(1-\gamma)d_1 + \gamma d_1(0)}. \qquad (9)$$

Note that eq.(9) also holds for $\gamma = 1$. Substitute p_{t1} from eq.(9) into eq.(8) and integrate. The parameters $\alpha = \frac{(1-\gamma)}{p_{t1}(0)}$ and $\beta = \frac{\gamma d_1(0)}{p_{t1}(0)} + 1$ are introduced to present the result with less clutter:

$$tk_A = \frac{\alpha}{\beta^2}\ln\left[\frac{\alpha d_1 + \beta}{\alpha d_1(0) + \beta}\right] + \frac{\beta - 1}{\beta}\left[\frac{1}{d_1} - \frac{1}{d_1(0)}\right] - \frac{\alpha}{\beta^2}\ln\left[\frac{d_1}{d_1(0)}\right]. \qquad (10)$$

This equation describes the decrease in d_1 with time and by eq.(9) the temporal behavior of p_{t1} also follows from eq.(10). The amount of DNA that has self-annealed (reaction 3c) is given by:

$$\frac{dD}{dt} = k_A d_1 d_2 = k_A d_1^2. \qquad (11)$$

When eq.(11) is integrated from $t = 0$ to $t = t_A$, the amount of DNA that has self-annealed, is found:

$$\int_0^D dD' = k_A \int_0^{t_A} d_1^2 dt.$$

Note that $D(0) = 0$, since the denaturation is complete. In order to determine the integral on the right, we again substitute p_{t1} from eq.(9) into eq.(8), re-arrange the terms and integrate it as follows:

$$-\int\left[\frac{\alpha d_1 + \beta - 1}{\alpha d_1 + \beta}\right] dd_1 = k_A \int d_1^2 dt = D.$$

After the integral on the left has been evaluated, the amount of DNA that has self-annealed is shown to have the following relation with d_1 for all $0 \le t \le t_A$:

$$D = d_1(0) - d_1 + \frac{1}{\alpha}\ln\left[\frac{\alpha d_1 + \beta}{\alpha d_1(0) + \beta}\right]. \qquad (12)$$

Thus D has an implicit relation with time, due to eq.(10). Also, eq.(12) is a balance over d_1;

$$d_1(0) = D + d_1 - \frac{1}{\alpha}\ln\left[\frac{\alpha d_1 + \beta}{\alpha d_1(0) + \beta}\right]$$ = *amount self-annealed (D) + amount not reacted (d_1) + amount that has formed annealed products with primer fragments, i.e.* $-\frac{1}{\alpha}\ln\left[\frac{\alpha d_1 + \beta}{\alpha d_1(0) + \beta}\right]$.

Thus the amount of $d_1(0)$ at the onset of the annealing step is distributed among the part that has self-annealed (D), the part that has not reacted (d_1) and the part that has reacted with primer or partial length fragments ($\sum_0^{N_A - 1} p1d(i)$). Let this last amount of anneal product be defined as $p1d_t(t_A) = \sum_0^{N_A - 1} p1d(i)$. Then it follows directly from eq.(12) that

$$p1d(t_A) = -\frac{1}{\alpha}\ln\left[\frac{\alpha d_1(t_A) + \beta}{\alpha d_1(0) + \beta}\right]. \qquad (13)$$

Now the annealed product distributions can be calculated, using the results of

eqns.(9,10,13).

The amount of primer1 of length *i* that has formed annealed complexes with DNA strands is found by pro-rating, using eq.(13):

$$p1d(i) = p1d_{t1}(t_A) \times p_1(i,0) / p_{t1}(0). \quad (14)$$

By the symmetry argument one finds that $p1d(i) = p2d(i)$. The fraction of primer1 that has been involved in primer-primer reactions is:

$$\alpha_p = \frac{p_{t1}(0) - p1d_t(t_A) - p_{t1}(t_A)}{p_{t1}(0)} \quad (15)$$

where eqns.(9,10) are used to determine the terms on the right hand side of eq.(15). The primer-primer distribution at the end of the annealing step is:

$$p12(i,j) = \alpha_p p_1(i,0) p_2(j,0) / p_{t1}(0). \quad (16)$$

Formation of ternary complexes. The formation of the ternary complex involves the assembly of the polymerase and the binary complex (primer:DNA). It is schematically depicted in Fig.3 (middle). The complexes $p1d(i)$, $p2d(i)$ and $p12(i,j)$ react with polymerase to form ternary complexes:

$$\begin{aligned} p1d(i) + \varepsilon &\rightarrow T1d(i) \\ p2d(i) + \varepsilon &\rightarrow T2d(i) \\ p12(i,j) + \varepsilon &\rightarrow T12(i,j) \end{aligned} \quad . \quad (17a\text{-}c)$$

The ternary complex formation takes place at the end of the annealing step. For the purpose of the model, we assign an assembly time for this process, t_{As}. The polymerase concentration at the start of the ternary complex formation is given by eq.(2). Note: since time has been reset at the beginning of the annealing step, we set $\varepsilon(t_A)$ during annealing equal to $\varepsilon(t_D)$ at the end of denaturation. The polymerase reacts with the annealed products as described by reactions (17a-c). The rate expression for these reactions, using the rate constant k_T, is:

$$\frac{d\varepsilon}{dt} = -k_T \left[\sum [p1d(i) + p2d(i)] + \sum\sum p12(i,j)\right] \times \varepsilon = -k_T pd_t \times \varepsilon. \quad (18)$$

The total amount of annealed product is denoted by pd_t and its value at the start of the assembly process is $pd_t(t_A)$, determined by eqns.(14,16). While the ternary complexes form, the following relation holds:

$\varepsilon(t_A) - \varepsilon(t) = pd_t(t_A) - pd_t(t)$, for $t \geq t_A$.

Introduce the constant $\hat{P} = pd_t(t_A) - \varepsilon(t_A)$ in the relation, then we can write: $pd_t(t) = \hat{P} + \varepsilon(t_A)$. Substitute this form for $pd_t(t)$ into eq.(18) and solve it. The amount of polymerase that has not bound to annealed product at the end of the assembly period is:

$$\varepsilon(t_{As}) = \frac{pol(t_A)\hat{P}e^{-k_T \hat{P} t_{As}}}{\varepsilon(t_A) + \hat{P} - \varepsilon(t_A)e^{-k_T \hat{P} t_{As}}}. \quad (19)$$

This result warrants some discussion. If the polymerase is in excess, then $\hat{P} < 0$. Despite lack of information about k_T and t_{As}, it is reasonable to assume the reactions are fast, therefore $-k_T \hat{P} t_{As} >> 1$ and the exponential terms in eq.(19) would dominate. In this case, eq.(19) gives the expected result:

$\varepsilon(t_{As}) = -\hat{P} = \varepsilon(t_A) - pd_t(t_A)$.

When the polymerase concentration is less than the total amount of annealed product,

$\hat{P} > 0$ and the exponential term in the denominator will be small compared to the other terms, thus

$$\varepsilon(t_{As}) = \frac{\varepsilon(t_A)\hat{P}e^{-k_T\hat{P}t_{As}}}{\varepsilon(t_A)+\hat{P}} \approx 0 .$$

In this case all the available polymerase has been used to form ternary complexes. The balance of annealed product does not form the ternary complex. A special case arises if $\hat{P} = 0$, since eq.(18) becomes a second order equation and solution (19) is not valid. However, if it is then assumed that $k_T t_{As} >> 1$, $\varepsilon(t_{As}) \approx 0$ and all $pd_t(t_A)$ would be converted to ternary complexes.

We define the fraction of $pd_t(t_A)$ that has formed ternary complexes as α_T. In light of the prior discussion, $\alpha_T = 1$ if $\hat{P} \le 0$ and $\alpha_T = \varepsilon(t_A)/\, pd_t(t_A)$ if $\hat{P} > 0$.

This result is used to find the values of the different ternary complexes:

$$T1d(i) = \alpha_T\, p1d(i)$$
$$T2d(i) = \alpha_T\, p2d(i) \quad . \qquad \text{(20a-c)}$$
$$T12(i,j) = \alpha_T\, p12(i,j)$$

To summarize, we have introduced the rate constant k_T and the assembly time t_{As}, but these additional parameters need not be known explicitly. The factor α_T is all we need and it is calculated from the polymerase and annealed product concentrations. This concludes the mathematical model of the annealing process.

d. Elongation

A systematic mechanism of the elongation chemistry is complex, but the essential reaction could be schematically presented as shown in Fig. 3 (bottom). The target strand and the annealed primer are shown at the left. In order to extend the complex by one base pair the correct dNTP precursor must be incorporated. The A, C, T and G are present as deoxynucleotide tri-phosphates (dNTP) but only the mono-phosphate is incorporated and inorganic pyrophosphate PP_i is produced. As the PP_i concentration increases, it competes with the dNTP's to adsorb at the growth site. Liu and Sommer (2004) have shown that type II DNA polymerases (e.g. KOD) also catalyze the pyrophosphorolysis reaction. If PP_i is adsorbed, the reverse reaction occurs; the complex is reduced by one base pair. The reversible reactions are included in the model. Another side reaction is thermal deamination of dCTP

$$dCTP + H_2O \Leftrightarrow dUTP + NH_3 .$$

This reaction transforms dCTP into dUTP (Connolly *et al*., (2003)). Thermal deamination of cytidine nucleotide increases about 5-fold for every 10°C increase in temperature above ambient. Theoretically this reaction is reversible, but the reverse step is a two-body process (dUTP + NH_3) and the volatile ammonia is usually present in low concentration. The equilibrium of the reaction shifts to the right with increased temperature. A brief motivation on our decision to use a stochastic approach for the elongation step would be helpful. All annealed products do not fully extend during the elongation step. Therefore a population distribution should be assigned to these partially extended fragments and the origin of this distribution is rooted in the competition between the dNTP's, PP_i and dUTP. A deterministic approach would have required a kernel, similar to the kernels which are used in particle fracture or droplet coalescence (Viljoen et al. (1990)), but the kernel would change from cycle to cycle as the concentrations of the competing species change.

An elongation time t_E is assigned to the process. Let v_E denote the average processing speed of the polymerase. In the case of *Taq pol*, $v_E \approx 110$ nt/s, for KOD pol, $v_E \approx 300$ nt/s. Viewed as a stochastic process, the speed v_E implies that a base pair is added (on the average) every $\Delta t_E = 1/(4v_E)$ seconds. This argument is based on excess (equi-molar) dNTP's in the solution. Therefore the number of events during elongation, i.e. attempts to add a base pair, is $4t_E v_E$. Consider a ternary complex $T1d(0)$. If n base pairs have been added to the complex after $4t_E v_E$ attempts, the ternary complex has been elongated to the target length $T1d(n)$. If fewer base pairs have been added over this period, a complex of intermediary length $T1d(j)$ is formed. This produces an intermediary primer $p_1(j)$ after denaturation that may elongate to target length during the next cycle. This is quite likely to occur, since only $n-j$ base pairs need to be added. The elongation of the ternary complex $T1d(0)$ in $4t_E v_E$ attempts is termed a statistical experiment. If this experiment is repeated many times, then the number of experiments that produces a certain length can be represented as a probability density function, $P(k)$. The moment of the PDF and the ternary complexes, $T1d(i)$, $T2d(i)$ and $T12(i,j)$ are calculated to find the product distribution after the elongation step.

Calculation of probability density function $P(k)$*.* Only the ternary complex $T1d(0)$ is used to calculate *P*(*k*) . This complex requires the longest extension. (Other complexes $T1d(m)$ would only require an extension of *n-m*.) The rationale is to calculate how far the extension will proceed for specific initial conditions (i.e. composition of solution at the start of that extension step) in the allotted time t_E.

The molar fractions of all reactants that can participate in elongation are written as:

$$y_i = \frac{\text{species } i}{dUTP + dATP + dGTP + dTTP + dCTP + PP_i}.$$

Species *i* represents any one of the species in the denominator. Suppose y_{dUTP}=0.02; y_{dCTP}=0.22; y_{dATP}=0.24; y_{dGTP}=0.24; y_{dTTP}=0.24 and y_{PP}=0.04. The molar fractions are arranged on a number line from zero to one:

$$0 \le y_{dUTP} \le 0.02 \le y_{dCTP} \le 0.24 \le y_{dATP} \le 0.48 \le y_{dGTP} \le 0.72 \le y_{dTTP} \le 0.96 \le y_{PP} \le 1$$

A random generator produces a number between zero and one and this determines the species that has arrived at the elongation site, with probability based on the molar fraction of each species. This species is compared to the species that must be incorporated (from DNA sequence data). If the correct species is selected, the complex $T1d(0)$ grows with one base pair, the selected dNTP is reduced by the amount $T1d(0)$, a similar amount of PPi is produced and the clock is advanced by Δt_E. At this stage the model is not adapted to address mutations. When a pyrophosphate is the selected species, (in the example above the random generator has produced a number between 0.96 and 1.00), the reverse phosphatase reaction occurs. The dNTP that matches the nucleic acid at the active site is increased by amount $T1d(0)$ and a similar amount of PPi is consumed and the clock is advanced by Δt_R. For the purpose of a qualitative model, the time steps for growth and regression are set equal. An exception is the case of dUTP. If dUTP is selected by the random generator, neither growth nor regression occurs, but a longer time step Δt_U is applied. In this model we have used $\Delta t_U = 2\Delta t_E$. The longer time step reflects the inhibitory

effect of dUTP. The process stops when the sum of time steps exceeds t_E. After time t_E, the complex has extended to $T1d(k)$, where in the case of $k = n$, the elongation has been completed.

When the simulation is repeated, a different extension may occur, due to the stochastic nature of this process. The simulation is repeated *M* times. The number of experiments that have produced a certain extension length is plotted as a function of the extension length. This plot represents the sum over independent 'experiments' (simulations). The central limit theorem (Freund (1972)) guarantees that a large number of simulations would approach a Gaussian distribution. This is the reason we have selected *M* = 5,000. After the plot has been normalized, the results are stored as $P(k)$. Thus $P(k)$ is a normalized distribution of the frequency of occurrences of all the possible complex sizes. The practical interpretation of the distribution is:
$P(k)$ = probability that a ternary complex adds *k* base pairs in time t_E for the given molar fractions y_i.

Example. In Fig.4 the distributions are shown for a 200 base pair amplicon and three different elongation times. The left plot corresponds to $t_E = 100\Delta t_E$, the middle curve shows the distribution for longer elongation time $t_E = 400\Delta t_E$ and the right curve shows the distribution for $t_E = 1{,}000\Delta t_E$. When larger *M* would be used, the distributions would be smoother, but it would become computationally more expensive. The Gaussian forms of shorter extension times are clearly distinguishable. In both shorter elongation time cases, the right hand sides of the distributions do not reach 200. Even for the distribution with $t_E = 400\Delta t_E$, the probability to fully extend a $T1d(0)$ complex is almost nil. The average of that distribution lies around 130 base pairs. Thus complexes $T1d(\geq 70)$ would most likely extend to $k = 200$. The distribution associated with $t_E = 1{,}000\Delta t_E$, reaches the target length of 200. Note that the magenta plot shows a sharp increase at $k = 200$ due to accumulation of product that has grown fully.

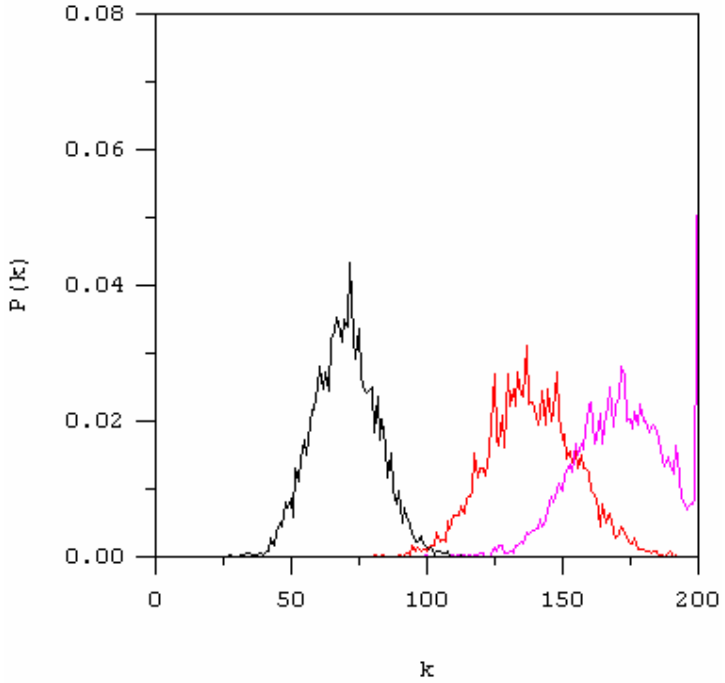

***Figure. 4:* Probability Distributions P(k)for three different extension times**

Implementation of $P(k)$. To keep the computational time within reason, the distribution $P(k)$ is calculated only once at the beginning of every elongation step. It is further understood that the set of ternary complexes consists of $\{T1d(j)_{0\le j\le n-1}, T2d(j)_{0\le j\le n-1}, T12(i,j)_{0\le i\le j; i\le j\le n-1}\}$. We define the discrete moment operator L that maps the set of ternary complexes into their extended products, denoted as Π. It is demonstrated for *T*1*d*(*j*):

$$L[T1d(j)] = (P(0)T1d(j); P(1)T1d(j)...P(n-j-1)T1d(j)...)$$
$$= (\Pi 1d(j); \Pi 1d(j+1); ...\Pi 1d(n-1); D; D..)$$

Note that $P(n-j-1)T1d(j)$ is still mapped into $\Pi(n-1)$, but $P(k)T1d(j)$ for $k \ge n-j$, is mapped into the fully extended amplicon *D*. To further illustrate this point, consider $T1d(90)$ in Fig.4. The fraction $T1d(90)\times P(0) = \Pi 1d(90)$ is that fraction of $T1d(90)$ that has not added a single base pair during t_E. Likewise $T1d(90)\times P(50)$ is the fraction that has grown to $\Pi 1d(140)$ and $T1d(90)\times \sum_{k\ge 110} P(k)$ will constitute the fraction that has grown to completion. In similar manner the complex $T2d(j)$ is mapped into $\Pi 2d$ and $T12(i,j)$ is mapped into $\Pi 12$. In the last case the product can only lie between $\Pi 12(i,j)$ and $\Pi 12(j,j)$ (remember the longer fragment is designated as *j*). The mapping procedure also records the amount with which each ternary complex is extended and it keeps track of the consumption of dNTP and production/consumption of pyrophosphate. After all mappings are complete, which marks the end of the elongation step, the concentrations of all species that compete for adsorption are updated. At the start of the next cycle this information is used to calculate an updated probability density distribution $P(k)$. This also concludes the last step in a PCR cycle.

4. Results

Comparison between theoretical and experimental results.

Case I: *E. coli* – 297 b.p. amplicon

Three different elongation times have been used with KOD polymerase; 1.8 s, 2.0 s and 2.2 s. When *Taq* pol is used, the elongation is considerably slower and an elongation time of 10 s is used. Amplicons have been amplified for 35 cycles with 0.2 s at 90°C (denaturation), 0.2 s at 58°C (annealing) and (1.8 s, 2.0 s and 2.2 s for KOD) and 10 s elongation for *Taq* at 72°C. The results are summarized in Table I. The yield with the KOD polymerase is significantly higher than with *Taq* pol. The mathematical model predicts yields that are close to the experimental values.

Table I: Summary of results for *E. coli* 297.

Theor. Yield	Exp. Yield	C_0	C_P	Cycles	Polymerase	Elongation time
87.8%	85.0%	1 pg	40 ng	33	KOD	1.8 s
45.3%	48.2%	1 ng	60 ng	35	*Taq*	10 s

Case II: *Bacillus cereus* – 600 b.p. amplicon

This amplicon has been amplified using KOD polymerase with a hot start of 30 sec at 90°C followed by 35 cycles of PCR and a temperature protocol of (0.2 s at 92°C, 0.2 s at 56°C and 2.0 s at 72°C). Two extension times, 12 s and 30 s, have been used for the

amplification of the 600 b.p. amplicon with *Taq* polymerase. All the samples have amplified but the yield has been better with 30 s elongation. We have used 35 cycles of PCR with (0.2 s at 92°C, 0.2 s at 56°C and 12 s and 30 s at 72°C).

Table II: Summary of results BC_4 600.

Theor. Yield	Exp. Yield	C_0	C_P	Cycles	Polymerase	Elongation time
76.9%	75.6%	1 pg	40 ng	35	KOD	2 s
36.8%	36.3%	10 ng	55 ng	35	*Taq*	12 s

The overall yields of the experiments and the mathematical model are summarized in Table II. It is noted that the theoretical values and the experimental results compare very well for both polymerases.

Case III: Bacteriophage λ – 2206 b.p. amplicon

The final system is λ- 2206 b.p. amplicon. PCR with the KOD polymerase gives higher yields when 10 s extension is used instead of 8 s. The amplicon has been amplified for 30 cycles of PCR run with (0.5 s at 90°C, 0.5 s at 58°C, and 8 s or 10 s at 72°C). In the case of amplification using *Taq* polymerase, the yield with 10 s extension time is only 22.5%. We have explored longer extension times, but to test the model we have purposefully selected conditions that will produce lower yields. The results of the experimental yields and theoretical yields are summarized in Table III. Again, the comparison between theoretical and experimental results is very good.

Table III: Summary of results of 2206bp λ_{DNA}.

Theor. Yield	Exp. Yield	C_0	C_P	Cycles	Polymerase	Elongation time
61.9%	57.8%	1 pg	40 ng	30	KOD	8 s
21.7%	22.5%	1 ng	20 ng	30	*Taq*	10 s

5. Discussion

A mathematical model of the PCR process has been presented. It has been divided into the three stages; DNA denaturing, primer annealing and elongation. Each stage has been described systematically. The primary value of a mathematical model is that it gives an analytical structure to the process; cause and effect becomes apparent so that parameter sensitivity, reaction conditions and reactant concentrations can be investigated. Six important findings of this study are summarized as follows.

1. Annealing is a two-step process that first involves the primer:template formation, followed by the ternary complex formation (primer:template:polymerase). The kinetics is fast and complete conversion occurs if primers and polymerase are in excess. These two factors render the need for exact kinetic parameters of the annealing process to be of lesser importance.
2. Yield varies from cycle to cycle. Incomplete enzymatic extension produces intermediary products that may extend completely during later cycles. Such incompklete DNA copying causes fluctuations in efficiency. A monotonic decrease in yield is indicative of reactant depletion and/or inhibition.
3. A probability density function is used to determine the products at the end of the extension step. The function is affected by reactant concentrations, the extension speed and the extension time.

4. The history of all species, including intermediary products, can be tracked through the entire process.
5. Extension rate is affected by species concentration. An interesting result of the model is that inhibition occurs when one deoxynucleotide triphosphate concentration is much higher than the rest, even though all four substrate dNTPs are in excess. For the experiments in section 2.1, 200 μM dNTP concentration is used. If one of the dNTP concentrations is increased significantly over the others, then the model predicts a significant drop in yield. Another interpretation is that disparate dNTP concentrations would lead to a slow-down in the effective extension rate. A kinetic study that utilizes this intentional slow-down is currently under investigation.
6. The average theoretical yields have been compared with experimental values for three different amplicons and two different polymerases. In all six cases the comparisons have been very good.

6. Notation

$A : A_{f,r}$ Arrhenius pre-exponential factor: forward and reverse pre-exponential factors

$C_{0,P}$ Initial and final product DNA concentrations

D Concentration of full target length double stranded DNA (dsDNA)

d_1, d_2 Concentration of full target length single stranded DNA (ssDNA)

$E : E_{f,r}$ Activation energy: forward and reverse activation energies

i, j, k Partially completed strand lengths

k_D Rate of polymerase thermal deactivation

k_A Annealing rate constant, primer/target and target/target

k_{eff} Fraction of polymerase not thermally deactivated

k_f, k_r Forward and reverse reaction rates

k_P Rate of primer/primer annealing

k_T Rate of tertiary complex formation

L Mapping operator

n Number of PCR cycles

N_C Complexity

$N_{T,A}$ Length of target or amplicon, measured in base pairs

$p(i, j)$ Population balance of primers *i* and *j*

$p_{1,2}(i)$ Concentration of primer1 or primer2 of length *i*

$p1,2d(i)$ Concentration of annealed product, consisting of primer1 or primer2 of length *i* and ssDNA

$p1,2d_L(k,i)$ Concentration that has grown to length *k*

$p1,2d_t$ Total concentration of primer/target complex, e.g. $p1d_t = \sum_{0}^{N_A-1} p1d(i)$.

$p12(i, j)$ Concentration of primer/primer complex

pd_t Total number of annealed products

p_{t1}, p_{t2} Total concentration of all primers and incomplete fragments. $p_{t1}(0), p_{t2}(0)$ denote values at the onset of an annealing step.

$P(v)$ Normalized extension rate distribution

$\hat{P}$ $pd_t(t_A) - \varepsilon(t_A)$

R Gas constant

S Shortest fragment length

$t : t_{A,As,E,D}$ Time: annealing time, annealing + polymerase assembly time, extension time, denaturation time

$T : T_D$ Temperature: denaturation temperature

$T1,2d(i), T12(i,j)$ Ternary complexes of $p1d(i), p2d(i), p12(i,j)$ respectively.

$v : v_E$ Extension rate: average extension rate

X Overall yield

Y Overall efficiency

y_i Molar fraction of species that may react during elongation

z Defined as ratio d_1 / p_{t1} .

Greek Symbols

α Defined as $(1-\gamma)/p_{t1}(0)$

α_P Fraction of primer involved in primer/primer complex, defined as $[p_{t1}(0) - p1d_t(t_A) - p_{t1}(t_A)]/p_{t1}(0)$.

α_T Fraction of annealed products that have formed a tertiary complex

β Defined as $[\gamma d_1(0)/p_{t1}(0)]+1$

γ Defined as the ratio of the two rate constants k_P / k_A .

$\Delta t : \Delta t_{As,E,R,U}$ Time step: tertiary complex assembly time, base pair extension time, pyrophosphatase reaction time, dUTP delay time

ε Polymerase enzyme concentration

$\Pi 1,2d, \Pi 12$ Extended products of ternary complexes

7. References

Connolly, B.A., *et al.*, (2003). Uracil recognition by archaeal family B DNA polymerases. Biochemical Society Transactions, 3, 699-702.

Freund, J.E. (1972). *Mathematical Statistics.* Prentice Hall, New York pp206-208

Gelfand DH and White TJ (1990) "Thermostable DNA Polymerases." In: MA Innis, DH Gelfand, JJ Sninsky, and TJ White, eds., PCR Protocols: a Guide to Methods and Applications, Academic Press, Inc., San Diego

Gilliland, G., (1990). Analysis of cytokine mRNA and DNA: detection and quantitation by competitive polymerase chain reaction. Proceedings of National Academy of Sciences, 87, 2725-2729.

Illanes, A., Wilson, L., (2003). Enzyme reactor design under thermal inactivation. Critical Reviews in Biotechnology, 23, 61-93.

Innis, MA, Myambo KB, Gelfand DH, and Brow MAD (1988) "DNA sequencing with *Thermus aquaticus* DNA polymerase and direct sequencing of polymerase chain-reaction amplified DNA." Proc. Nat. Acad. Sciences USA **85**: 9436-9440.

Johnson B (1998) "The Competition Heats Up. The annual review of thermal cyclers takes a sneak peak at the new products for 1998." The Scientist, 12 (24): "Thermal Block Table."

Kainz, P. (2000). The PCR Plateau phase – towards an understanding of its limitations, Biochimica et Biophysics Acta, 1494 23-27.

Keohavong, P., *et al*., (1988). Laboratory methods DNA amplification *in vitro* using T4 DNA polymerase. DNA, 7, 63-70.

Li, H., *et al*., (1988). Amplification and analysis of DNA sequences in single human sperm and diploid cells. Nature, 335, 414-417.

Liu, Q., Sommer, S.S., (2004) Pyrophosphorolysis by Type II DNA polymerases: implications for pyrophosphorolysis-activated polymerization. Analytical Biochemistry, 324, 22-28.

Mizuguchi H, Nakatsuji M, Fujiwara S, Takagi M, Imanaka T. (1999). Characterization and application to hot start PCR of neutralizing monoclonal antibodies against KOD DNA polymerase. J. Biochem. 126. 762-768.

Mullis, K.B., Faloona, F.A., (1987). Specific Synthesis of DNA *in vitro* via a polymerase-catalyzed chain reaction. Methods in Enzymology, 155, 335-350.

Newton, C.R., Graham, A. (1997). PCR Second Edition. Springer, Oxford, pp. 1-8.

Nicoll S, Brass A, and Cubie HA (2001) “Detection of herpes viruses in clinical samples using real-time PCR.” J. Virol. Methods **96**: 25-31.

Oste CC (1989) “PCR Automation.” In: Erlich HA, ed., PCR Technology: Principles and Applications for DNA Amplification, Stockton Press, New York, pp. 23-30.

Oste CC (1994) "PCR Instrumentation: Where Do We Stand?" In: K Mullis, F Ferré, and RA Gibbs, eds. (1994) The Polymerase Chain Reaction, Birkhauser, Boston, pp.165-173.

Quintanar A and Nelson RM (2002) “A process and apparatus for high-speed amplification of DNA.” U.S. Patent No. 6,472,186.

Saiki RK, Scharf S, Faloona F, Mullis KB, Horn GT, Erlich HA and Arnheim N (1985) “Enzymatic amplification of beta-globin genomic sequences and restriction site analysis for diagnosis of sickle cell anemia.” Science. 230. 1350-1354

Schnell, S., Mendoza, C. (1997) Enzymological Considerations for a Theoretical Description of the Quantitative Competitive Polymerase Chain Reaction (QC-PCR), J. theor. Biol. 184, 433-440.

Schnell, S., Mendoza, C. (1997) Theoretical Description of the Polymerase Chain Reaction, J. theor. Biol. 188, 313-318.

Smith, J.M. (1981) *Chemical Engineering Kinetics*, McGraw-Hill, New York.

Stolovitzky, G. Cecchi, G. (1996). Efficiency of DNA replication in the polymerase chain reaction, Proc. Nat. Acad. Sci. USA 93, 12947-12952.

Viljoen, H.J., D. Eyre and C.J. Wright (1990) "Solving Dynamic Equations for the Collection and Evaporation of an Aerosol", Can. J. Chem. Eng. 68, 938-943.

Waterfall, C.M., Eisenthal, R., Cobb, B.D. (2002). Kinetic characterization of primer mismatches in allele-specific PCR: a quantitative assessment. Biochem. Biophys. Res. Commun. 299, 715-722.

Whitney, S., R. Agupally, R, M. Nelson, and H.J.Viljoen, ``Principles of the Polymerase Chain Reaction: Mathematical Modeling and Experimental Verification'' Comp. Biol & Chem. **28** pp195-209 (2004).